© 2021. Published by The Company of Biologists Ltd | Journal of Cell Science (2021) 134, jcs255950. doi:10.1242/jcs.255950

SHORT REPORT

Human cells lacking CDC14A and CDC14B show differences in ciliogenesis but not in mitotic progression

Patrick Partscht[1,2], Borhan Uddin[1,*] and Elmar Schiebel[1,‡]

ABSTRACT

The budding yeast phosphatase Cdc14 has a central role in mitotic exit and cytokinesis. Puzzlingly, a uniform picture for the three human CDC14 paralogues CDC14A, CDC14B and CDC14C in cell cycle control has not emerged to date. Redundant functions between the three CDC14 phosphatases could explain this unclear picture. To address the possibility of redundancy, we tested expression of *CDC14* and analysed cell cycle progression of cells with single and double deletions in *CDC14* genes. Our data suggest that *CDC14C* is not expressed in human RPE1 cells, excluding a function in this cell line. Single- and double-knockouts (KO) of *CDC14A* and *CDC14B* in RPE1 cells indicate that both phosphatases are not important for the timing of mitotic phases, cytokinesis and cell proliferation. However, cycling *CDC14A* KO and *CDC14B* KO cells show altered ciliogenesis compared to wild-type cells. The cilia of cycling *CDC14A* KO cells are longer, whereas *CDC14B* KO cilia are more frequent and disassemble faster. In conclusion, this study demonstrates that the cell cycle functions of CDC14 proteins are not conserved between yeast and human cells.

KEY WORDS: Human CDC14, Mitosis, Cytokinesis, DNA damage, Ciliogenesis

INTRODUCTION

CDC14 encodes an essential highly conserved dual specificity protein phosphatase that in budding yeast *Saccharomyces cerevisiae* promotes mitotic exit, the transition from mitosis into G1 phase, and cytokinesis (Taylor et al., 1997). During most of the cell cycle, *S. cerevisiae* Cdc14 is entrapped in the nucleolus by complex formation with the protein Net1 (also known as Cfi1) (Shou et al., 1999; Visintin et al., 1999). With anaphase onset, Cdc14 becomes released from the nucleolus in two waves. The Cdc14 early anaphase release (FEAR) pathway, consisting of the polo-like kinase Cdc5, the kinetochore protein Slk19, Spo12 and the cohesion regulator separase, triggers a partial release of Cdc14 that leads to the dephosphorylation of spindle associated proteins and of the kinase Cdc15 (Jaspersen and Morgan, 2000; Stegmeier et al., 2002). Cdc15 is a component of the mitotic exit network (MEN), a GTPase-driven signalling cascade that controls Cdc14 after FEAR (Pereira et al., 2000). MEN activation of Cdc14 then promotes mitotic exit and cytokinesis through the dephosphorylation of cyclin-dependent kinase (CDK1) sites in proteins that trigger cyclin B degradation or play a role in anaphase spindle formation and cytokinesis (Jaspersen et al., 1999; Palani et al., 2012; Raspelli et al., 2015; Bremmer et al., 2012). In addition, the fission yeast Cdc14 orthologue Clp1 (also known as Flp1) is entrapped in the nucleolus during interphase; however, it is released by prophase, and thus earlier in the cell cycle than Cdc14 (Cueille et al., 2001). As for *S. cerevisiae* Cdc14, fission yeast Clp1 controls cytokinesis (Trautmann et al., 2001). An additional cell cycle function of Clp1/Flp1 is at the spindle pole body (SPB) where Clp1/Flp1 participates in an activation loop triggering Cdc25 activation and mitotic entry (Chan et al., 2017; Esteban et al., 2004; Wolfe and Gould, 2004).

The human genome encodes for three *CDC14* genes, named human *CDC14A*, *CDC14B* and *CDC14C* (Mailand et al., 2002; Mocciaro and Schiebel, 2010). *CDC14C* is a near pseudogene of *CDC14B* and only differs in a small number of bases from *CDC14B* cDNA (Rosso et al., 2008). CDC14A and CDC14B vary by a 54-amino-acid long N-terminal extension in CDC14B that is important for the targeting of this protein to the nucleolus during interphase (Kaiser et al., 2002). Functions for the human CDC14 phosphatases that have been suggested are DNA damage control, cell cycle regulation, regulation of the primary cilia and the actin cytoskeleton (Mocciaro and Schiebel, 2010; Uddin et al., 2018). Loss of CDC14A function in humans is associated with deafness and infertility, indicating an important role of this phosphatase in the inner ear and testis (Imtiaz et al., 2018). A systematic study on substrates that are dephosphorylated by CDC14A identified components of the actin cytoskeleton, such as the protein eplin (also known as LIMA1) (Chen et al., 2017, 2016). CDC14B substrates are not as well characterized.

Do human CDC14 paralogues have cell cycle functions, as this is the case for yeast CDC14 phosphatases? Based on a gene knockout (KO) for human *CDC14B* it was concluded that it is dispensable for chromosome segregation and mitotic exit (Berdougo et al., 2008). However, it was never tested whether functional redundancy between the three CDC14 paralogues masks cell cycle functions. Here, we show that *CDC14C* is not expressed in human retina epithelial cells immortalized with hTERT (RPE1) cells. RPE1 cells with genomic inactivation (knockout; KO) of the *CDC14A*, *CDC14B* and *CDC14A CDC14B* show no mitotic or other severe cell cycle defects. However, knockout of *CDC14A* or *CDC14B* impacts ciliogenesis of cycling cells, although in different ways. These data suggest that the functions of CDC14 phosphatases diverged during evolution from essential cell cycle regulation of mitosis in budding yeast to more divergent functions centred on the actin cytoskeleton and cilia in higher eukaryotes.

RESULTS AND DISCUSSION

CDC14C is not expressed in human RPE1 cells

Redundancy between *CDC14* paralogues could mask functions upon inactivation of only one *CDC14* gene, for example in cell

[1]Zentrum für Molekulare Biologie, Universität Heidelberg, DKFZ-ZMBH Allianz, Heidelberg 69120, Germany. [2]Heidelberg Biosciences International Graduate School (HBIGS), Universität Heidelberg, Heidelberg, Germany.
*Present address: Department of Biochemistry and Molecular Biology, Jahangirnagar University, Dhaka, Bangladesh.

‡Author for correspondence: e.schiebel@zmbh.uni-heidelbeg.de

P.P., 0000-0002-8766-3901; B.U., 0000-0001-9142-7568; E.S., 0000-0002-3683-247X

Handling Editor: David Glover
Received 17 October 2020; Accepted 10 December 2020

Journal of Cell Science (2021) 134, jcs255950. doi:10.1242/jcs.255950

cycle regulation. A prerequisite for redundancy is the co-expression of *CDC14* genes. In order to judge this, we first analysed transcription of *CDC14* genes in tissues and cell lines using published databases. This indicated that *CDC14C* is only transcribed in testis and brain but not in other organs, whereas *CDC14A* and *CDC14B* are expressed in almost all tissues (Brawand et al., 2011) (Fig. 1A). In line with this finding, RNA sequencing using the non-transformed telomerase-immortalized cell line RPE1 derived from retina did not identify *CDC14C* transcripts, while *CDC14A* and *CDC14B* mRNAs were detected (Fig. 1B (Santaguida et al., 2015)). To confirm that the *CDC14C* gene is not expressed in RPE1 cells, we analysed *CDC14C* mRNA by RT-PCR and DNA sequencing. This analysis was complicated by the fact that the DNA sequence of the chromosomal copy of *CDC14C* is very similar to the cDNA of *CDC14B* (Fig. 1C, red stars indicate differences). To avoid amplifying the chromosomal *CDC14B*, we choose specific primers that amplified the cDNA of *CDC14B* and *CDC14C*, and genomic *CDC14C*, but not genomic *CDC14B* due to the large size (26.348 bp) of this genome-specific *CDC14B* PCR product (Fig. 1C, see panel I). To judge expression of *CDC14B* and *CDC14C* and to exclude contamination with genomic *CDC14C* DNA, we treated the mRNA before the RT-PCR with and without DNaseI. Without DNaseI incubation, the RT-PCR combined with DNA sequencing identified the *CDC14B* and *CDC14C* signatures (Fig. 1C, see panel II). With DNaseI treatment, however, only the *CDC14B* signature was detected (Fig. 1C, see panel III) suggesting that the *CDC14C* PCR product in the absence of DNaseI arose from genomic DNA. To exclude that *CDC14C* expression is upregulated by the loss of *CDC14A* and *CDC14B*, we analysed *CDC14C* transcripts in *CDC14A* and *CDC14B* double-KO (hereafter *CDC14A/B* KO) cells. Only *CDC14B* but not *CDC14C* mRNA was detected in this experiment (Fig. 1C, see panel IV). This indicates that *CDC14C* is not expressed in cycling RPE1 cells while *CDC14A* and *CDC14B* are expressed.

Mitosis is undisturbed in RPE1 cells lacking *CDC14A* and *CDC14B*

The main function of budding yeast Cdc14 is in the regulation of anaphase events and mitotic exit (Mocciaro and Schiebel, 2010). In mammalian cells, this function of CDC14 is mainly taken over by the phosphatases PP1 and PP2 (Cundell et al., 2013; Holder et al., 2019). However, because of the lack of a systematic study on cell cycle progression on cells with impaired CDC14A and CDC14B function, it is still possible that CDC14 phosphatases control aspects of mitosis. Because of the lack of *CDC14C* expression in RPE1 cells (Fig. 1B,C), we focused the analysis on *CDC14A* and *CDC14B*. To avoid misinterpretations from incomplete siRNA depletions, we inactivated *CDC14A* and *CDC14B* by genomic gene deletion (see Materials and Methods). We addressed mitotic functions of CDC14A and CDC14B by analysing transition times of mitotic phases from live-cell imaging data of wild-type (WT), *CDC14A* KO (AKO6), *CDC14B* KO (BKO10) and *CDC14A/B* KO (BAKO3) RPE1 cell lines expressing the chromatin marker *H2B-mNG*. We did not observe changes in the timing of the transition in the timing of the transition from prometaphase to metaphase, metaphase to anaphase onset and prometaphase to anaphase onset in any of the deletion cell lines compared to the WT control (Fig. 2A,B). In addition, analysis of the timing of actin ring contraction did not indicate a role of the CDC14A and CDC14B phosphatases in the regulation of cytokinesis (Fig. 2C,D), in contrast to what was observed previously in *Caenorhabditis elegans* embryos (Gruneberg et al., 2002). Finally, we analysed mitotic exit by arresting cells in prometaphase using the microtubule depolymerizing drug nocodazole, followed by nocodazole washout and analysis of progression of cells into G1 (Fig. 2E, top). No difference between WT and *CDC14* KO cells was observed for mitotic exit (Fig. 2E, bottom). Thus, in human RPE1 cells CDC14A and CDC14B phosphatases do not have obvious mitotic functions.

Loss of *CDC14A* or *CDC14B* function does not affect cell proliferation

Because of the lack of mitotic defects, we asked whether CDC14A and CDC14B have a more general role in the cell growth and division. We first tested whether cell proliferation was affected when cells lacked *CDC14A* or *CDC14B*. This was done with the MTT [3-(4,5-dimethylthiazole-2-yl)-2,5-diphenyltetrazolium bromide] assay, which measures the activity of the enzyme NAD(P)H-dependent cellular oxidoreductase and therefore reflects fitness and proliferation of cells (Mosmann, 1983). Analysis of the MTT profiles of RPE1 cells with single and double-deletion of *CDC14A* and *CDC14B* did not indicate a proliferation difference of the *CDC14* mutants in comparison to WT RPE1 (Fig. 3A). To measure the cell doubling more directly, we covalently labelled intracellular proteins with a pulse of the fluorescent cell division tracker dye carboxyfluorescein succinimidyl ester (CFSE) (Chung et al., 2017). The decrease in CFSE intensity due to growth and cell division was monitored by flow cytometry. The CFSE signal decreased similarly for WT and *CDC14* (AKO6, BKO10, BAKO3) cells (Fig. 3B). The protein Ki-67 (also known as MKI67) is a marker for cell proliferation (Gerdes et al., 1983). A similar percentage of WT and *CDC14* KO cells were Ki-67 positive (Fig. 3C) suggesting that most cells are dividing. This is consistent with the results from the MTT and CFSE assays, and together indicates that CDC14A and CDC14B are not important for growth and division of RPE1 cells.

In order to detect cell cycle differences between WT and *CDC14* KO RPE1 cells, we analysed cycling RPE1 cells by flow cytometry using propidium iodide and phospho-histone H3 antibodies as a mitosis marker. This did not indicate major differences in the cell cycle distribution between WT and *CDC14* KO cells (Fig. 3D–F).

Taken together, loss of CDC14A and CDC14B does not significantly alter the cell proliferation rate, cell cycle distribution and the mitotic index, which is consistent with our finding that mitotic progression and mitotic exit is undisturbed (Fig. 2).

Cycling *CDC14A* and *CDC14B* KO RPE1 cells show distinct ciliogenesis phenotypes

Despite high conservation, human CDC14 phosphatases appear to play a role in more divergent biological processes when compared to the mitotic functions in yeast. Loss of function analysis of *CDC14A* and *CDC14B* in mice and DT40 cells suggests both CDC14 paralogues have a role of in DNA repair (Lin et al., 2015; Mocciaro et al., 2010; Wei et al., 2011). In addition, depletion of CDC14A and CDC14B in zebrafish suggests a role in ciliogenesis (Clement et al., 2011, 2012). We previously observed longer cilia in serum starved *CDC14* KO RPE1 cells (Uddin et al., 2018).

To test whether deletion of *CDC14* genes in RPE1 cells leads to the accumulation of DNA damage and affects ciliogenesis, we analysed cycling *CDC14* KO cells for both phenotypes using appropriate markers. *CDC14A* and *CDC14B* single- and double-KO cells showed an increase in the number of nuclear phospho-H2AX (S139) foci (Fig. S1A,B), which appear in response to double-strand breaks (Rogakou et al., 1998). Moreover, loss of *CDC14A* and *CDC14B*

Journal of Cell Science (2021) 134, jcs255950. doi:10.1242/jcs.255950

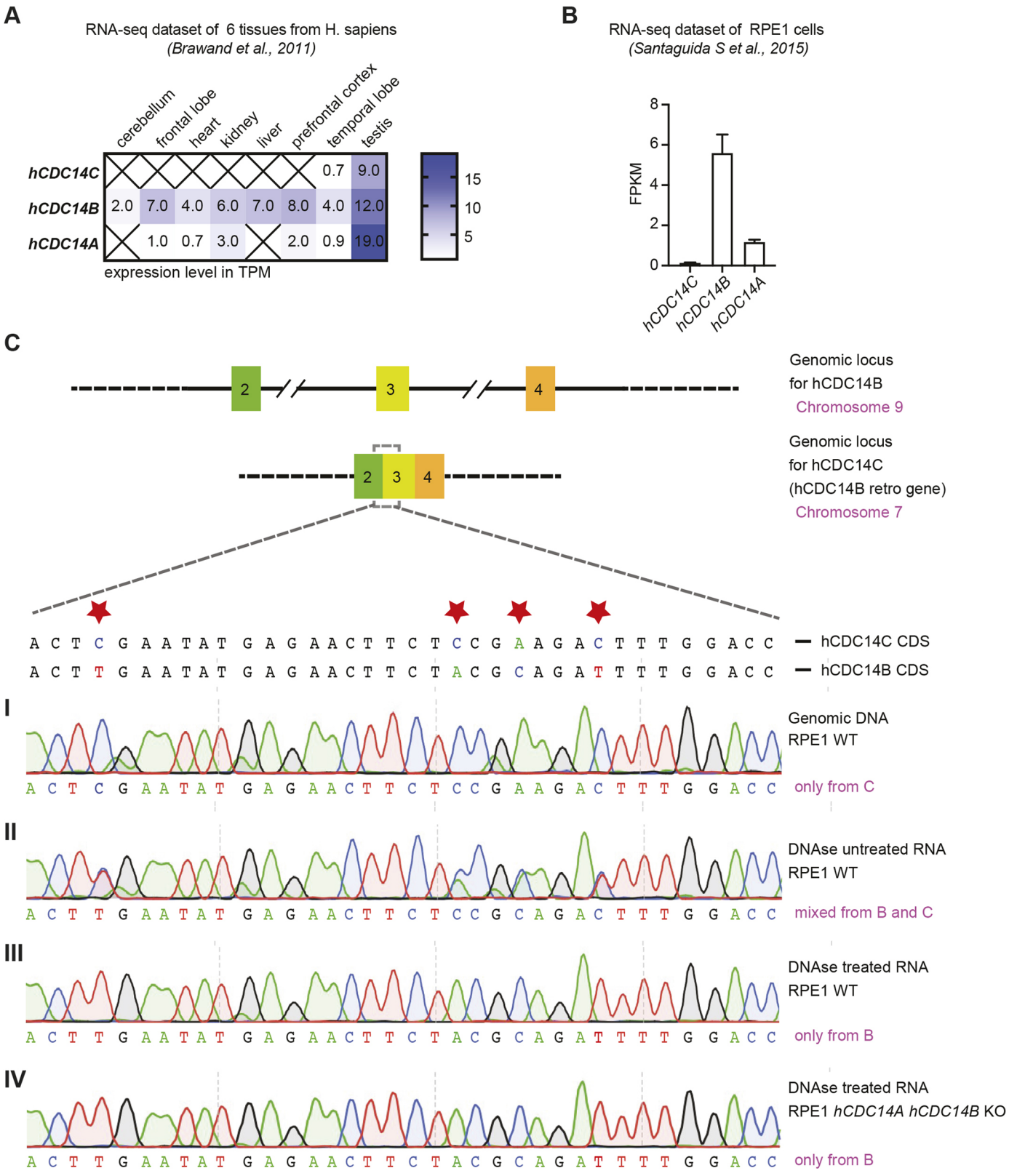

Fig. 1. Transcription analysis of *CDC14A*, *CDC14B* and *CDC14C*. (A) Transcripts per million (TPM) expression values of *CDC14* genes from RNA-sequencing dataset of six human organs (Brawand et al., 2011). (B) Fragments per kilobase million (FPKM) expression values of the *CDC14* isoforms from the RNA-sequencing dataset (Santaguida et al., 2015). (C) RT-PCR and DNA sequence analysis demonstrate that *CDC14C* is not expressed in RPE1 WT cells. Red stars mark bases that are different between *CDC14B* and *CDC14C*. (C, panel I) PCR with chromosomal DNA identified only *CDC14C*. (C, panel II) cDNA was prepared by RT-PCR without DNaseI treatment. The RT-PCR combined with DNA sequence analysis identified the signatures of *CDC14C* and the cDNA of *CDC14B*. (C, panel III) RT-PCR product analysis after DNaseI treatment from RPE1 WT cells showed expression of *CDC14B*, but not *CDC14C*. (C, panel IV) cDNA from *CDC14A*/*B* KO cells was prepared by RT-PCR with DNaseI treatment. *CDC14C* is not expressed in these cells.

Journal of Cell Science (2021) 134, jcs255950. doi:10.1242/jcs.255950

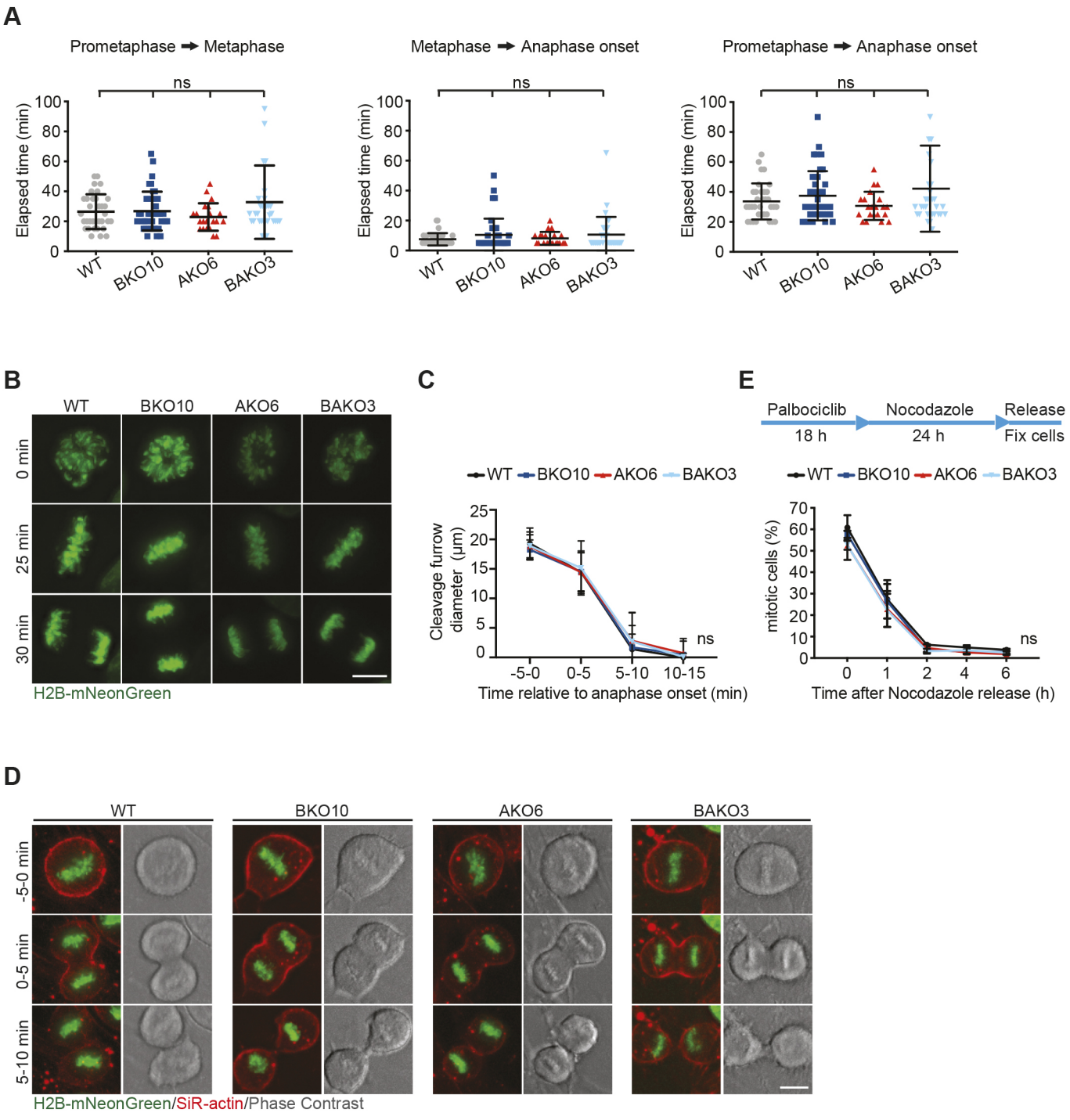

Fig. 2. Deletion of *CDC14A*, *CDC14B* and *CDC14A*/*B* does not affect mitosis and cytokinesis. (A) Mitotic progression of RPE1 WT and *CDC14* KO cells (AKO6, *CDC14A* KO; BKO10, *CDC14B* KO; BAKO3, *CDC14B* and *CDC14A* double KO) stably expressing histone *H2B-mNG* were analysed by time-lapse live cell imaging. Elapsed time between prometaphase (nuclear envelope breakdown), metaphase (alignment of chromosomes at the spindle equator) and early anaphase (first movement of chromosomes towards spindle poles) was determined. Images were captured every 5 min. Results are mean±s.d. (N=3, n>20 cells). (B) Images of RPE1 cells progressing through different stages of mitosis. (C) H2B–mNeonGreen-expressing RPE1 WT and *CDC14* KO cells were stained with SiR–actin to monitor the diameter of the contractile ring by time-lapse live-cell imaging relative to anaphase onset (t=0). Results are mean±s.d. (N=3, n>30 cells). (D) Images of SiR–actin-stained cytokinetic RPE1 cells with indicated genotypes during cytokinesis. (E) RPE1 WT and *CDC14* KO cells were enriched in prometaphase by blocking cells in G1 with palbociclib incubation and palbociclib washout, followed by nocodazole treatment. After washing out nocodazole, cells were collected at the depicted time points and mitotic exit kinetic was assessed by flow cytometry using antibodies against serine 10 in histone H3. Results are mean±s.d. (N=3, n=30,000 events). Results are ns [one-way ANOVA followed by Tukey's test (A), two-way ANOVA followed by Tukey's test (C,E)]. Scale bars: 10 µm.

affected ciliogenesis in RPE1 KO cells. Approximately 6% of cycling WT and *CDC14A* KO cells and 15% of *CDC14B* KO and *CDC14A/B* KO cells carried cilia (Fig. 4A,C). The average cilia length of WT and *CDC14B* KO (BKO10) cells was 1.6 µm. The length in *CDC14A* KO (AKO6) and *CDC14A/B* KO (BAKO3) cells was with 2 µm significantly longer (Fig. 4B,C).

Journal of Cell Science (2021) 134, jcs255950. doi:10.1242/jcs.255950

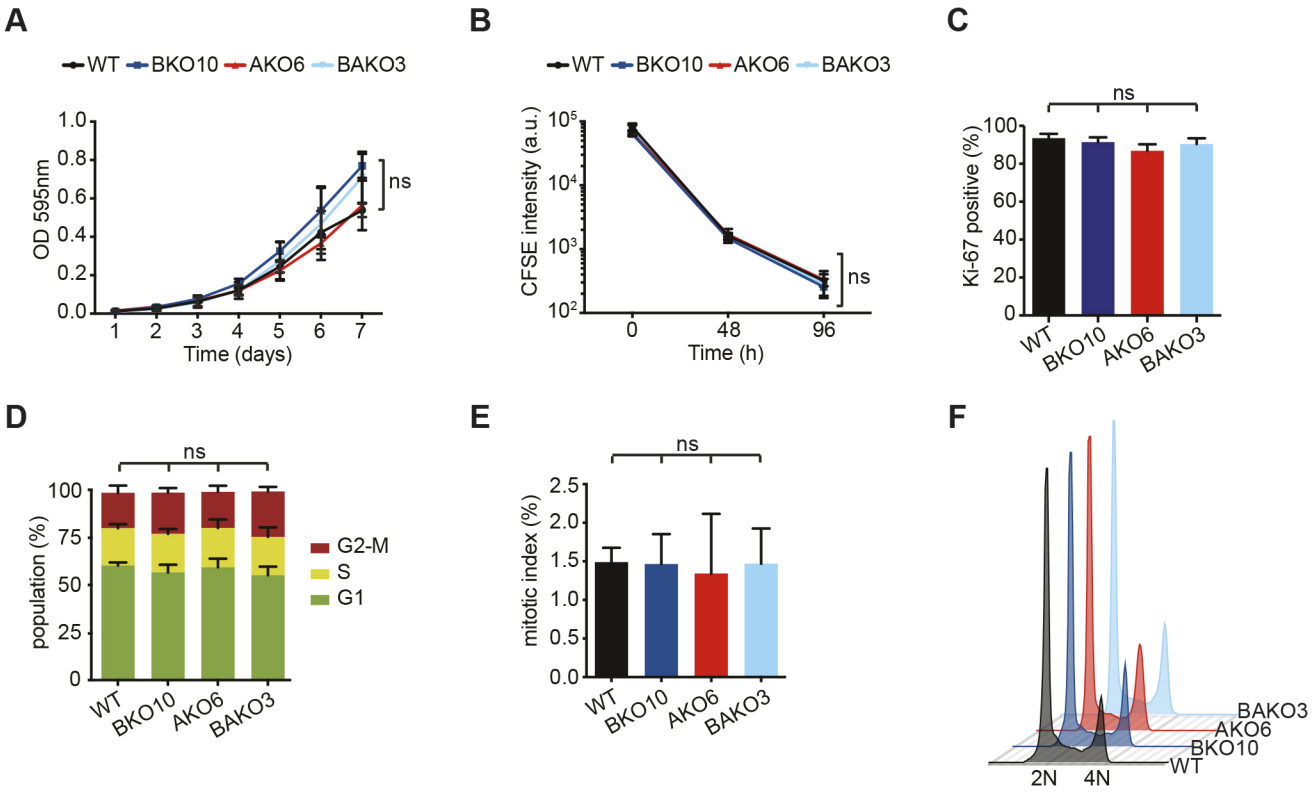

Fig. 3. *CDC14A/B* KO cells show normal proliferation and cell cycle distribution. (A) Metabolic activity reflecting growth rate of RPE1 WT and *CDC14* KO (AKO6, *CDC14A* KO; BKO10, *CDC14B* KO; BAKO3, *CDC14B* and *CDC14A* double KO) cells was assessed by MTT colorimetric assay. Results are mean±s.d. (*N*=3). (B) Decreasing CFSE intensity reflecting cell division was monitored by flow cytometry. Results are mean±s.d. (*N*=4, *n*=40,000 events). (C) The expression of the proliferation marker Ki-67 was determined by immunofluorescence microscopy to assess the proportion (%) of RPE1 cells in the population that were growing for each of the indicated genotypes. Results are mean±s.d. (*N*=3, *n*>150 cells). (D,E) Flow cytometric analysis (%) of cell cycle distribution by quantification of DNA content after propidium iodide staining (D) and by assessment of the mitotic index using antibodies specific for phospho-histone $H3^{pS10}$ (E). Results are mean±s.d. (*N*=4, *n*=40,000 events). (F) Representative propidium iodide histograms from flow cytometry analysis in D, demonstrating comparable DNA content profiles between the cell populations with indicated genotypes. Results are ns [two-tailed unpaired *t*-test (A,B), one-way ANOVA followed by Tukey's test (C), two-way ANOVA followed by Tukey's test (D,E)].

Replicating RPE1 cells are able to assemble a primary cilium in G1 phase (Spalluto et al., 2013). To test whether this is also the case in the RPE1 *CDC14* KO cell lines, we arrested the cell cycle of RPE1 cells in G1 using the CDK4–cyclin D inhibitor palbociclib (Trotter and Hagan, 2020) in the presence of serum and measured formation and properties of cilia. In these conditions, 20% of the RPE1 WT and *CDC14A* KO cells and 30% of the *CDC14B* KO and *CDC14A/B* KO cells formed cilia (Fig. 4D,E), which is 2–4-times more frequently than in cycling cells (Fig. 4A). As observed for cycling cells, the cilia from *CDC14A* KO and *CDC14A/B* KO cells were longer than those from WT and *CDC14B* KO cells (Fig. 4F). Importantly, after the release from the G1 block by palbociclib washout *CDC14B* KO and *CDC14A/B KO* cells disassembled their cilia three times faster than WT and *CDC14A* KO cells (Fig. 4G).

Complementation of *CDC14* KO cells by rescue constructs is complicated by the fact that *CDC14* overexpression has a strong impact on cell cycle progression, centrosome duplication and cell division (Kaiser et al., 2002; Mailand et al., 2002; Uddin et al., 2018). To confirm the DNA damage and cilia phenotype of *CDC14A* and *CDC14B* KO cells, we used independently constructed *CDC14* KO RPE1 cell lines (AKO7, BKO17 and BAKO20) that showed the same accumulation of phospho-H2AX foci (Fig. S2A) and the same difference in cilia number, length and disassembly (Fig. S2B–D) than the first cohort of cell lines. In summary, the lack of *CDC14A* and *CDC14B* leads to the accumulation of DNA damage and impacts cilia formation in G1 phase and their subsequent disassembly in later cell cycle phases.

The molecular cause of the accumulation of phospho-H2AX foci and the altered ciliogenesis regulation in *CDC14* KO RPE1 cells is currently unclear and needs further investigation. Previously, we have shown that in serum starved cells, the phospho-regulation of actin-binding protein drebrin by the cyclin-dependent kinase CDK5 and the phosphatase CDC14A contributes to cilia length regulation (Maskey et al., 2015; Uddin et al., 2018). Furthermore, the CDK10 and cyclin M protein kinase, whose deficiency is linked to STAR syndrome, have been reported to negatively regulate ciliogenesis (Guen et al., 2018, 2016). It is therefore conceivable that CDC14A or CDC14B also counteract members of the CDK kinase family in some process of ciliogenesis during interphase.

MATERIALS AND METHODS

Cell culture and treatments

hTERT-RPE1 cells were cultured in Gibco DMEM/F-12 (Gibco) medium supplemented with 10% FBS, 1% L-glutamine and 1% penicillin/streptomycin at 37°C with 5% CO_2. Cells were routinely tested for mycoplasma contamination. RPE1 cells were treated for 18 h with 100 nM palbociclib (Tocris cat. #4786) to arrest cells in G1. To arrest cells in prometaphase, cells were first arrested in G1 with palbociclib for 18 h, followed by palbociclib washout and treatment with 330 nM nocodazole for 24 h.

Journal of Cell Science (2021) 134, jcs255950. doi:10.1242/jcs.255950

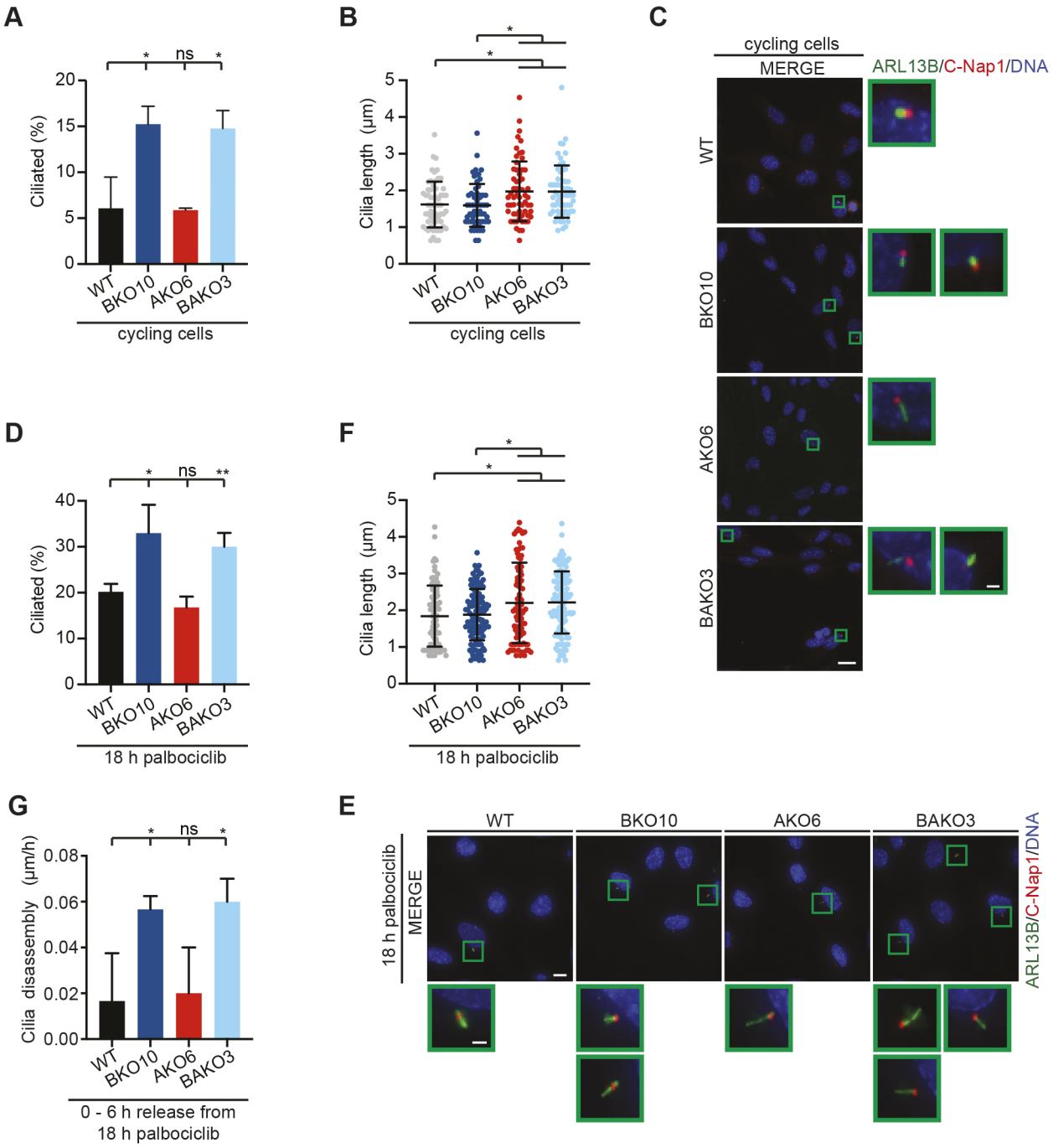

Fig. 4. Absence of functional *CDC14A*/*B* phosphatase genes leads to altered cilia regulation in cycling cells. (A,B) To observe the ciliation behaviour in cycling RPE1 WT and *CDC14* KO (AKO6, *CDC14A* KO; BKO10, *CDC14B* KO; BAKO3, *CDC14B* and *CDC14A* double KO) cells, we stained for the ciliary marker ARL13B and quantified the number of ciliated cells (A) and cilia length (B). Results are mean±s.d. (N=3, n>300 cells). (C) Representative immunofluorescence images from experiments in A and D. (D,F) Ciliation efficiency (D) and cilia length (F) of RPE1 WT and *CDC14* KO cells upon treatment with palbociclib for 18 h. Results are mean±s.d. (N=3, n>150 cells). (E) Representative immunofluorescence images from experiments in D and F. (G) Cells synchronized in G1 from D–F were monitored 0 and 6 h after release from palbociclib using immunofluorescence microscopy. Cilia disassembly rates were assessed from subtracting the mean cilia length at t=0 and t=6 h. Results are mean±s.d. (N=3, n>150 cells). Results are ns; *P≤0.05 [two-tailed unpaired t-test (A,D,G); one-way ANOVA followed by Tukey's test (B,F)]. Scale bars: 20 µm (C); 10 µm (E) (main images), 2 µm (magnified views, C,E).

Generation of KO cell lines

RPE1 *CDC14B*, *CDC14A* single KO and *CDC14A/B* KO cell lines were generated previously by zinc finger nuclease-based approaches and confirmed by southern blotting, RT-PCR and sequencing (Chen et al., 2017, 2016; Uddin et al., 2015). In brief, exon 9 of *CDC14A* was targeted to generate a deletion of 77 amino acids (203–279 aa) around the catalytic cysteine residue. *CDC14B* KO cells were generated by Cre-recombinase-mediated removal of the selection marker leading to incorporation of premature stop codons in all three frames immediately followed by a single loxP site (34 bp) at exon 4 upstream of the catalytic site. *CDC14A* KO was carried out on top of Cre-infected *CDC14B* KO cells to obtain double-KO cells.

Generation of stable cell lines

H2B–mNeonGreen-expressing cell lines were generated via retroviral gene transfer according to manufacturer's protocol (Clontech) using the construct pQCXIZ-H2B-mNeonGreen. Stable cells constitutively expressing the construct were enriched by fluorescence-activated cell sorting using a BD FACS Aria III instrument (Beckton Dickinson).

RT-PCR and sequence analysis

Total RNA was isolated from cells using the RNeasy Mini Kit (Qiagen, Hilden, Germany) following the manufacturer's instructions. RT-PCR analysis were carried out using SuperScript® III One-Step RT-PCR System with Platinum® Taq DNA Polymerase (Invitrogen). Sequencing was carried out after gel purification of the PCR products. PCR primer sequences used to amplify the sequence flanking exon 2 and exon 7 of CDC14B/C were 5'-GCCATTCTCTACAGCAG-3′ and 5'-GGAAGCCATACTGCATTGC-3′. The results of our sequence analysis were compared with publicly available RNA sequencing data banks (Brawand et al., 2011; Santaguida et al., 2015). The utilized datasets are available at NCBI GEO under accession codes GSE30352 and GSE60570, respectively.

MTT assay

Cells were counted three times and 3×10^4 cells were resuspended in 8 ml cell medium. 750 cells were seeded into 96-well in quadruplicates for each time point and grown up to 7 days. Every 24 h, cell viability/proliferation was assayed by replacing cell medium with medium containing freshly prepared MTT (5 mg/ml MTT in PBS diluted 1:10 in cell medium). After 3.5 h at 37°C, MTT medium was carefully removed and formazan crystals were dissolved in 100 µl 2-propanol for 2 h while shaking. MTT reduction was quantified at an absorbance of 595 nm using the M1000 plate reader (Tecan).

CFSE proliferation assay

For CFSE staining, a CellTrace™ CFSE Cell Proliferation Kit (Thermo Fisher) was used according to manufacturer's protocol. Stained cells (5×10^4) were seeded in six-well plates and grown for up to 4 days before fixation with 4% PFA in PBS for 10 min at room temperature. The CFSE intensity of fixed cells was assessed by flow cytometry (BD Canto II).

Flow cytometry

For analysis of cell cycle distribution and mitotic index, cells were washed once with PBS and fixed with 70% ethanol in phosphate-buffered saline (PBS) at −20°C for 3 h. Fixed cells were permeabilized with 0.25% Triton X-100 for 15 min on ice before staining with anti-phospho-histone H3 (Ser10) (rabbit, 1:1000, Cell Signaling #3377S) overnight at 4°C. Then, cells were washed with PBS containing 1% BSA and stained with fluorescently labelled (Alexa Fluor 488) anti-rabbit-IgG secondary antibody (Invitrogen, A-21206, 1:500) for 30 min at room temperature. Cells were washed with PBS and treated with RNase A (100 µg/ml) at 37°C in dark for 30 min. Immediately before flow cytometric analysis (BD Canto), propidium iodide staining solution (25 µg/ml) was added.

Immunofluorescence microscopy

Cells were seeded on coverslips and allowed to attach overnight before treatment. Depending on the primary antibody, cells were fixed with 4% PFA in PBS (10 min at room temperature) or with methanol (5 min at −20°C). Fixed cells were permeabilized with 0.1% Triton X-100 in PBS for 10 min at room temperature and incubated with 10% FBS for 1 h at room temperature to block non-specific antibody binding. Next, cells were incubated with primary antibody for 1 h. Then, cells were incubated with the secondary antibody and the DNA dye Hoechst 33342 (1:2000) for 30 min. Coverslips were mounted with Moviol and dried overnight. Images were acquired on a DeltaVision RT system (Applied Precision) equipped with an Olympus IX71 microscope. The following antibodies were used in immunofluorescence microscopy (IF) experiments: $H2AX^{pS139}$ (rabbit, 1:1000, Cell Signaling #9718), Ki-67 (mouse, 1:100, Santa Cruz Biotechnology sc-23900), C-Nap1 (goat, 1:1000, Panic et al., 2015), ARL13B (rabbit, 1:200, Proteintech 17711-1-AP), Alexa Fluor 488/555/647 (mouse/rabbit/sheep/goat, 1:500, Invitrogen).

Live-cell fluorescence imaging

Live-cell imaging was performed using a DeltaVision RT system (Applied Precision) with an Olympus IX71 microscope at 37°C. Cells were seeded in Ibidi glassware and cultured in DMEM/F-12 complete medium with HEPES and without Phenol Red (Gibco). If applicable, cell medium was supplemented with 100 nM SiR-actin (Lukinavičius et al., 2014) (Spirochrome) and labelled for 6 h before imaging. Time-lapse images were collected at 5 min intervals.

Statistical analysis

If not otherwise stated, results were confirmed by three independent experiments (n=3) and are expressed as mean±s.d. Prism 8 software (GraphPad) was used for statistical significance analysis including two-tailed unpaired Student's t-test and one-way or two-way ANOVA followed by Tukey's multiple comparison test (ns, $P>0.05$; *$P\leq0.05$; **$P\leq0.01$; ***$P\leq0.001$; ****$P\leq0.0001$).

Acknowledgements

We thank Dr Monika Langlotz (Heidelberg) for the FACS experiments and Dr Iain Hagan (Manchester) for communicating data before publication. Some of the content from Fig. 1 in this paper formed part of Borhan Uddin's PhD thesis in the Combined Faculties for the Natural Sciences and for Mathematics at the Ruperto-Carola University of Heidelberg in 2018.

Competing interests

The authors declare no competing or financial interests.

Author contributions

Conceptualization: E.S.; Investigation: P.P., B.U.; Writing - original draft: E.S., P.P.; Writing - review & editing: P.P.; Supervision: E.S.

Funding

This work was supported by Deutsche Forschungsgemeinschaft grant Schi295/3-4.

Supplementary information

Supplementary information available online at
https://jcs.biologists.org/lookup/doi/10.1242/jcs.255950.supplemental

Peer review history

The peer review history is available online at
https://jcs.biologists.org/lookup/doi/10.1242/jcs.255950.reviewer-comments.pdf

References

Berdougo, E., Nachury, M. V., Jackson, P. K. and Jallepalli, P. V. (2008). The nucleolar phosphatase Cdc14B is dispensable for chromosome segregation and mitotic exit in human cells. *Cell Cycle* **7**, 1184-1190. doi:10.4161/cc.7.9.5792

Brawand, D., Soumillon, M., Necsulea, A., Julien, P., Csardi, G., Harrigan, P., Weier, M., Liechti, A., Aximu-Petri, A., Kircher, M. et al. (2011). The evolution of gene expression levels in mammalian organs. *Nature* **478**, 343-348. doi:10.1038/nature10532

Bremmer, S. C., Hall, H., Martinez, J. S., Eissler, C. L., Hinrichsen, T. H., Rossie, S., Parker, L. L., Hall, M. C. and Charbonneau, H. (2012). Cdc14 phosphatases preferentially dephosphorylate a subset of cyclin-dependent kinase (Cdk) sites containing phosphoserine. *J. Biol. Chem.* **287**, 1662-1669. doi:10.1074/jbc.M111.281105

Chan, K. Y., Alonso-Nuñez, M., Grallert, A., Tanaka, K., Connolly, Y., Smith, D. L. and Hagan, I. M. (2017). Dialogue between centrosomal entrance and exit scaffold pathways regulates mitotic commitment. *J. Cell Biol.* **216**, 2795-2812. doi:10.1083/jcb.201702172

Chen, N.-P., Uddin, B., Voit, R. and Schiebel, E. (2016). Human phosphatase CDC14A is recruited to the cell leading edge to regulate cell migration and adhesion. *Proc. Natl. Acad. Sci. USA* **113**, 990-995. doi:10.1073/pnas.1515605113

Chen, N.-P., Uddin, B., Hardt, R., Ding, W., Panic, M., Lucibello, I., Kammerer, P., Ruppert, T. and Schiebel, E. (2017). Human phosphatase CDC14A regulates actin organization through dephosphorylation of epithelial protein lost in neoplasm. *Proc. Natl. Acad. Sci. USA* **114**, 5201-5206. doi:10.1073/pnas.1619356114

Chung, S., Kim, S.-H., Seo, Y., Kim, S.-K. and Lee, J. Y. (2017). Quantitative analysis of cell proliferation by a dye dilution assay: application to cell lines and cocultures. *Cytometry A* **91**, 704-712. doi:10.1002/cyto.a.23105

Clement, A., Solnica-Krezel, L. and Gould, K. L. (2011). The Cdc14B phosphatase contributes to ciliogenesis in zebrafish. *Development* **138**, 291-302. doi:10.1242/dev.055038

Clement, A., Solnica-Krezel, L. and Gould, K. L. (2012). Functional redundancy between Cdc14 phosphatases in zebrafish ciliogenesis. *Dev. Dyn.* **241**, 1911-1921. doi:10.1002/dvdy.23876

Cueille, N., Salimova, E., Esteban, V., Blanco, M., Moreno, S., Bueno, A. and Simanis, V. (2001). Flp1, a fission yeast orthologue of the S-cerevisiae CDC14 gene, is not required for cyclin degradation or rum1p stabilisation at the end of mitosis. *J. Cell Sci.* **114**, 2649-2664.

Cundell, M. J., Bastos, R. N., Zhang, T., Holder, J., Gruneberg, U., Novak, B. and Barr, F. A. (2013). The BEG (PP2A-B55/ENSA/Greatwall) pathway ensures cytokinesis follows chromosome separation. *Mol. Cell* **52**, 393-405. doi:10.1016/j.molcel.2013.09.005

Esteban, V., Blanco, M., Cueille, N., Simanis, V., Moreno, S. and Bueno, A. (2004). A role for the Cdc14-family phosphatase Flp1p at the end of the cell cycle in controlling the rapid degradation of the mitotic inducer Cdc25p in fission yeast. *J. Cell Sci.* **117**, 2461-2468. doi:10.1242/jcs.01107

Gerdes, J., Schwab, U., Lemke, H. and Stein, H. (1983). Production of a mouse monoclonal antibody reactive with a human nuclear antigen associated with cell proliferation. *Int. J. Cancer* **31**, 13-20. doi:10.1002/ijc.2910310104

Gruneberg, U., Glotzer, M., Gartner, A. and Nigg, E. A. (2002). The CeCDC-14 phosphatase is required for cytokinesis in the Caenorhabditis elegans embryo. *J. Cell Biol.* **158**, 901-914. doi:10.1083/jcb.200202054

Guen, V. J., Gamble, C., Perez, D. E., Bourassa, S., Zappel, H., Gärtner, J., Lees, J. A. and Colas, P. (2016). STAR syndrome-associated CDK10/Cyclin M regulates actin network architecture and ciliogenesis. *Cell Cycle* **15**, 678-688. doi:10.1080/15384101.2016.1147632

Guen, V. J., Edvardson, S., Fraenkel, N. D., Fattal-Valevski, A., Jalas, C., Anteby, I., Shaag, A., Dor, T., Gillis, D., Kerem, E. et al. (2018). A homozygous deleterious CDK10 mutation in a patient with agenesis of corpus callosum, retinopathy, and deafness. *Am. J. Med. Genet. A* **176**, 92-98. doi:10.1002/ajmg.a.38506

Holder, J., Poser, E. and Barr, F. A. (2019). Getting out of mitosis: spatial and temporal control of mitotic exit and cytokinesis by PP1 and PP2A. *FEBS Lett.* **593**, 2908-2924. doi:10.1002/1873-3468.13595

Imtiaz, A., Belyantseva, I. A., Beirl, A. J., Fenollar-Ferrer, C., Bashir, R., Bukhari, I., Bouzid, A., Shaukat, U., Azaiez, H., Booth, K. T. et al. (2018). CDC14A phosphatase is essential for hearing and male fertility in mouse and human. *Hum. Mol. Genet.* **27**, 780-798. doi:10.1093/hmg/ddx440

Jaspersen, S. L. and Morgan, D. O. (2000). Cdc14 activates Cdc15 to promote mitotic exit in budding yeast. *Curr. Biol.* **10**, 615-618. doi:10.1016/S0960-9822(00)00491-7

Jaspersen, S. L., Charles, J. F. and Morgan, D. O. (1999). Inhibitory phosphorylation of the APC regulator Hct1 is controlled by the kinase Cdc28 and the phosphatase Cdc14. *Curr. Biol.* **9**, 227-236. doi:10.1016/S0960-9822(99)80111-0

Kaiser, B. K., Zimmerman, Z. A., Charbonneau, H. and Jackson, P. K. (2002). Disruption of centrosome structure, chromosome segregation, and cytokinesis by misexpression of human Cdc14A phosphatase. *Mol. Biol. Cell* **13**, 2289-2300. doi:10.1091/mbc.01-11-0535

Lin, H., Ha, K., Lu, G., Fang, X., Cheng, R., Zuo, Q. and Zhang, P. (2015). Cdc14A and Cdc14B redundantly regulate DNA double-strand break repair. *Mol. Cell. Biol.* **35**, 3657-3668. doi:10.1128/MCB.00233-15

Lukinavičius, G., Reymond, L., D'Este, E., Masharina, A., Göttfert, F., Ta, H., Güther, A., Fournier, M., Rizzo, S., Waldmann, H. et al. (2014). Fluorogenic probes for live-cell imaging of the cytoskeleton. *Nat. Methods* **11**, 731-733. doi:10.1038/nmeth.2972

Mailand, N., Lukas, C., Kaiser, B. K., Jackson, P. K., Bartek, J. and Lukas, J. (2002). Deregulated human Cdc14A phosphatase disrupts centrosome separation and chromosome segregation. *Nat. Cell Biol.* **4**, 317-322. doi:10.1038/ncb777

Maskey, D., Marlin, M. C., Kim, S., Kim, S., Ong, E. C., Li, G. and Tsiokas, L. (2015). Cell cycle-dependent ubiquitylation and destruction of NDE1 by CDK5-FBW7 regulates ciliary length. *EMBO J.* **34**, 2424-2440. doi:10.15252/embj.201490831

Mocciaro, A. and Schiebel, E. (2010). Cdc14: a highly conserved family of phosphatases with non-conserved functions? *J. Cell Sci.* **123**, 2867-2876. doi:10.1242/jcs.074815

Mocciaro, A., Berdougo, E., Zeng, K., Black, E., Vagnarelli, P., Earnshaw, W., Gillespie, D., Jallepalli, P. and Schiebel, E. (2010). Vertebrate cells genetically deficient for Cdc14A or Cdc14B retain DNA damage checkpoint proficiency but are impaired in DNA repair. *J. Cell Biol.* **189**, 631-639. doi:10.1083/jcb.200910057

Mosmann, T. (1983). Rapid colorimetric assay for cellular growth and survival: application to proliferation and cytotoxicity assays. *J. Immunol. Methods* **65**, 55-63. doi:10.1016/0022-1759(83)90303-4

Panic, M., Hata, S., Neuner, A., Schiebel, E. (2015). The centrosomal linker and microtubules provide dual levels of spatial coordination of centrosomes. *PLOS Genetics* **11**, e1005243. doi:10.1371/journal.pgen.1005243

Palani, S., Meitinger, F., Boehm, M. E., Lehmann, W. D. and Pereira, G. (2012). Cdc14-dependent dephosphorylation of Inn1 contributes to Inn1-Cyk3 complex formation. *J. Cell Sci.* **125**, 3091-3096. doi:10.1242/jcs.106021

Pereira, G., Hofken, T., Grindlay, J., Manson, C. and Schiebel, E. (2000). The Bub2p spindle checkpoint links nuclear migration with mitotic exit. *Mol. Cell* **6**, 1-10. doi:10.1016/S1097-2765(05)00017-1

Raspelli, E., Cassani, C., Chiroli, E. and Fraschini, R. (2015). Budding yeast Swe1 is involved in the control of mitotic spindle elongation and is regulated by Cdc14 phosphatase during mitosis. *J. Biol. Chem.* **290**, 6006. doi:10.1074/jbc.A114.590984

Rogakou, E. P., Pilch, D. R., Orr, A. H., Ivanova, V. S. and Bonner, W. M. (1998). DNA double-stranded breaks induce histone H2AX phosphorylation on serine 139. *J. Biol. Chem.* **273**, 5858-5868. doi:10.1074/jbc.273.10.5858

Rosso, L., Marques, A. C., Weier, M., Lambert, N., Lambot, M.-A., Vanderhaeghen, P. and Kaessmann, H. (2008). Birth and rapid subcellular adaptation of a hominoid-specific CDC14 protein. *PLoS Biol.* **6**, e140. doi:10.1371/journal.pbio.0060140

Santaguida, S., Vasile, E., White, E. and Amon, A. (2015). Aneuploidy-induced cellular stresses limit autophagic degradation. *Genes Dev.* **29**, 2010-2021. doi:10.1101/gad.269118.115

Shou, W., Seol, J. H., Shevchenko, A., Baskerville, C., Moazed, D., Chen, W. S., Jang, J., Shevchenko, A., Charbonneau, H. and Deshaies, R. (1999). Exit from mitosis is triggered by Tem1-dependent release of the protein phosphatase Cdc14 from nucleolar RENT complex. *Cell* **97**, 233-244. doi:10.1016/S0092-8674(00)80733-3

Spalluto, C., Wilson, D. I. and Hearn, T. (2013). Evidence for reciliation of RPE1 cells in late G1 phase, and ciliary localisation of cyclin B1. *FEBS Open Biol.* **3**, 334-340. doi:10.1016/j.fob.2013.08.002

Stegmeier, F., Visintin, R. and Amon, A. (2002). Separase, polo kinase, the kinetochore protein Slk19, and Spo12 function in a network that controls Cdc14 localization during early anaphase. *Cell* **108**, 207-220. doi:10.1016/S0092-8674(02)00618-9

Taylor, G. S., Liu, Y., Baskervillie, C. and Charbonneau, H. (1997). The activity of Cdc14p, an oligomeric dual specific protein phosphatase from *Saccharomyces cerevisiae*, is required for cell cycle progression. *J. Biol. Chem.* **272**, 24054-24063. doi:10.1074/jbc.272.38.24054

Trautmann, S., Wolfe, B. A., Jorgensen, P., Tyers, M., Gould, K. L. and McCollum, D. (2001). Fission yeast Clp1p phosphatase regulates G2/M transition and coordination of cytokinesis with cell cycle progression. *Curr. Biol.* **11**, 931-940. doi:10.1016/S0960-9822(01)00268-8

Trotter, E. W. and Hagan, I. M. (2020). Release from cell cycle arrest with Cdk4/6 inhibitors generates highly synchronised cell cycle progression in human cell culture. *Open Biol.* **10**, 200200. doi:10.1098/rsob.200200

Uddin, B., Chen, N.-P., Panic, M. and Schiebel, E. (2015). Genome editing through large insertion leads to the skipping of targeted exon. *BMC Genomics* **16**, 1082. doi:10.1186/s12864-015-2284-8

Uddin, B., Partscht, P., Chen, N. P., Neuner, A., Weiss, M., Hardt, R., Jafarpour, A., Hessling, B., Ruppert, T., Lorenz, H. et al. (2018). The human phosphatase CDC14A modulates primary cilium length by regulating centrosomal actin nucleation. *EMBO Rep.* **20**, e46544. doi:10.15252/embr.201846544

Visintin, R., Hwang, E. S. and Amon, A. (1999). Cfi1 prevents premature exit from mitosis by anchoring Cdc14 phosphatase in the nucleolus. *Nature* **398**, 818-823. doi:10.1038/19775

Wei, Z., Peddibhotla, S., Lin, H., Fang, X., Li, M., Rosen, J. M. and Zhang, P. (2011). Early onset aging and defective DNA damage response in Cdc14b-deficient mice. *Mol. Cell. Biol.* **31**, 1470-1477. doi:10.1128/MCB.01330-10

Wolfe, B. A. and Gould, K. L. (2004). Fission yeast Clp1p phosphatase affects G2/M transition and mitotic exit through Cdc25p inactivation. *EMBO J.* **23**, 919-929. doi:10.1038/sj.emboj.7600103